

Optical Spectroscopy of Hydrogenic Atoms

MIT Department of Physics

This experiment is an exercise in optical spectroscopy in a study of the spectra of “hydrogenic” atoms, i.e. atoms with one “optical” electron outside a closed shell of other electrons. Measurement of the Balmer lines of atomic hydrogen and the fine structure of sodium lines; determination of the mass of the deuteron from the isotope shift. A reflection grating spectrograph is used to study the Balmer lines of hydrogen and the more complex hydrogenic spectrum of sodium, using the mercury spectrum as the wavelength calibrator. The measured Balmer wavelengths are compared with the quantum theory of the hydrogen spectrum, and a value of the Rydberg is derived. The transitions responsible for the sodium spectrum are identified, and the regularities in the fine structure and adherence to the selection rules are observed. A research grade monochromator is used to measure the isotope shift between the Balmer lines of hydrogen and deuterium, and the ratio of the deuteron mass to the proton mass is derived from the data.

PREPARATORY QUESTIONS

1. Construct as complete an energy level diagram of atomic hydrogen as you can, and show the transitions that give rise to the Balmer lines. (Incidentally, just exactly what is a spectral “line”?)
2. Read sections 2.1–2.7, 6.2.1 and 6.2.4 in the Richardson Grating Laboratory’s *Diffraction Grating Handbook 4th Edition* available at www.gratinglab.com and define the following terms: *grating equation, diffraction orders, angular dispersion, linear dispersion, resolving power, spectral resolution, bandpass, focal length, f/#, and free-spectral range.*
3. Suppose perfectly monochromatic light of wavelength 5000 \AA enters a reflection grating spectrograph (see description of the instrument below) with the slit width set at $10.0 \mu\text{m}$, and suppose the beam fully illuminates the concave grating which is a $3 \text{ cm} \times 3 \text{ cm}$ square with $1200 \text{ lines mm}^{-1}$. Make a plot with properly scaled axes of the light intensity versus angular displacement in the focal plane of the spectrograph in the first order diffracted image of the slit. Show quantitatively the salient features of the multiple slit diffraction pattern. (see Hecht 1998 Section 10.2.3)
4. Throughout this experiment the tabulated wavelengths of the mercury spectrum will be used as the calibration reference. Suppose, however, you had to start from scratch with no reference wavelengths. How would you establish an absolute scale of wavelengths?
5. Predict the isotope shift in wavelength (i.e., the difference in wavelength $\Delta\lambda = \lambda_H - \lambda_D$) of the first 3 Balmer lines of hydrogen and deuterium.

INTRODUCTION

The study of the optical spectra of hydrogen and other atoms having a single “optically active” electron in a spherically symmetric potential was specially important in the development of modern physics because of the simplicity of the spectra and the clarity with which their features could be understood in terms of the developing theories of quantum electrodynamics and atomic structure. The purpose of this experiment is to acquaint you with some of these features and with some of the methods of optical spectroscopy through an investigation of the spectra of hydrogen, deuterium, and the alkali metals.

Bohr’s theory of the optical spectrum of hydrogen, published in 1913, opened the door to the modern theory of atomic structure. In 1912 Bohr had come to Rutherford’s Laboratory at Manchester University where the concept of the atomic nucleus had been invented the previous year by Rutherford in his theory of the scattering of alpha particles by thin metal foils. Bohr immediately began to wrestle with the problem of how electrons in orbit about a nucleus can constitute a stable system when the classical laws of electromagnetism imply they must radiate their orbital energy and spiral into the nucleus. Bohr concluded that new, non-classical physical principles must govern atomic phenomena. By the summer of 1912 he arrived at his central idea that some form of quantization restricts the orbits of electrons inside atoms. He had in mind the quantum idea introduced by Planck in 1900 in his theory of the spectrum of blackbody radiation and invoked by Einstein in 1905 to explain the photoelectric effect. Then somebody brought to Bohr’s attention the simple regularities of the hydrogen spectrum, expressed in the formula discovered by Balmer in 1885. Afterward he said, “As soon as I saw Balmer’s formula the whole thing was immediately clear to me” (Rhodes 1986).

The Balmer spectrum of atomic hydrogen is readily produced by an electrical discharge in molecular hydro-

gen (H_2) at low pressure. The resulting collisions of mildly energetic electrons with hydrogen molecules cause dissociations of the molecules and excitations of the resulting atoms to states which decay in transitions that yield the Balmer lines in the visible region of the spectrum, as well as the Lyman lines in the ultraviolet, and other series of lines in the infrared. **Measurement of the Balmer lines, verification of the Balmer/Bohr formula for their wavelengths, and determination of the Rydberg constant are the first objectives of this experiment.**

Interesting variations on the theme of the hydrogen spectrum are found in the spectra of other single-electron atoms such as deuterium, tritium, singly ionized helium, doubly ionized lithium, all the way up to 25-times ionized iron. One expects the spectra of these atoms to be similar to that of hydrogen except for the effects of changes in the reduced mass, the nuclear charge, and the hyperfine interactions between the electronic and nuclear magnetic moments. In the laboratory it is difficult to produce a sufficient density of excited, multiply-ionized helium or lithium to yield a detectable spectrum of their single-electron ion species. As for hydrogen-like iron, it has only been seen in the radiation from solar flares, neutron stars in accreting binary systems, and the hot intergalactic gas in clusters of galaxies. But the effect on the spectrum of a change in the reduced mass of the nucleus-electron system is readily observed in deuterium. **Measurement of this “isotope” shift in the Balmer lines and determination of the ratio of the mass of the deuteron to the mass of the proton is another objective of this experiment.**

Another kind of “hydrogenic” spectrum is produced by atoms with one electron outside of “closed” shells. Examples are the alkali metals, singly-ionized alkaline earth metals, doubly-ionized elements in the third column of the periodic chart, etc. In such an atom or ion a single “optical” electron moves in the spherically symmetric potential of the nucleus and the closed shells of the inner electrons, and the eigenstates and energy eigenvalues of the atom can be calculated, in principle, as perturbed solutions of the Schrödinger equation for a hydrogen-like atom with a perturbation potential that represents the distortion of the simple $1/r$ potential of a point nucleus by the inner electrons. One effect of this shielding is to enhance the splitting of the levels with angular momentum quantum numbers $L > 0$ due to the spin-orbit interaction. Measurements of the doublet separations provide clues to the identity of the states involved in the transitions that give rise to the lines. **A third objective of this experiment is the measurement of the doublet separations of the spectral lines of sodium and the identification of the quantum transitions responsible for the lines.**

Most of the theoretical background you need for understanding the atomic spectra to be measured in this exper-

iment is the Appendices and in Chapter 2 of Melissinos (1966). More thorough treatments can be found in your texts for 8.04 and 8.05. Another useful and classic reference is *Introduction to Atomic Spectra* by C. F. White (1934). Here we will concentrate on describing the features of the equipment and procedures peculiar to the setups in Junior Lab.

EXPERIMENTAL APPARATUS

Two different spectroscopic instruments will be used in this investigation. The first is a commercially available 1/8 m reflection grating **spectrograph** (Thermo Oriel MS-125) with which you can record broad spectra at moderate resolution (2.2\AA) using a 2048 linear-element charged coupled device (CCD) array (Thermo Oriel Linespec). The second instrument is a research grade high-resolution (0.03\AA) scanning **monochromator** (Jobin Yvon 1250M) with a maximum resolving capacity $R_{max} = \lambda/\Delta\lambda \approx 10^4$. It will be used to measure the isotope shift between the Balmer lines of hydrogen and deuterium as well as the energy splittings due to the interaction between the electron spin and its orbital angular momentum ($\vec{L} \cdot \vec{S}$ coupling).

Both instruments utilize what is known as a Czerny-Turner mount. In this configuration, light from a source is focused onto an input slit through which it expands to fill a concave spherical mirror at a distance equal to the focal length of the instrument. The collimated light then is reflected onto a plane reflection grating (held fixed in the spectrograph and rotated in the monochromator) and from there the dispersed light is reflected to a second spherical concave mirror. This final mirror refocuses the light at the position of the exit aperture (spectrograph) or slit (monochromator) where the photons are detected and integrated.

THE GRATING SPECTROGRAPH

The grating spectrograph is illustrated in Figure 1. It has an interchangeable slit assembly ($10\mu\text{m}$, $100\mu\text{m}$, and $1000\mu\text{m}$ slit widths are available) followed by a concave spherical mirror which collimates the light onto a plane reflection grating with 1200 grooves mm^{-1} and which is $30\text{mm} \times 30\text{mm}$ square. The dispersed image of the slit is then refocused by the second concave spherical mirror onto a CCD array of 2048 pixels, each of which is $14\mu\text{m}$ wide by $200\mu\text{m}$ high. Its focal length f is 120mm and it has a low F/number = 3.7 and thus relatively good light gathering capacity (for a diffuse source, the throughput flux goes as $\phi \propto \frac{1}{F/\#^2}$). You can examine the interior of the instrument by removing the 5 screws to the light-tight lid and prying it open with a dime or screwdriver. **If you wish to replace the 1200 groove mm^{-1} grating**

with one of greater or lesser groove density, please ask an instructor for assistance. The grating is expensive and its surface is vulnerable to damage. Do not touch the grating surface with your fingers or with the edge of the grating cover. Use latex gloves to keep the oils from your skin from getting on the grating surface.

Mount the $100\mu\text{m}$ slit with the shiny side towards the light source, in the spectrograph entrance aperture. For greater or lesser resolution, $10\mu\text{m}$ and $1000\mu\text{m}$ slits are available on the optical table near the spectrograph. Mount the mercury discharge tube in the black power supply and place it ~ 10 inches away from the input slit. It should emit strongly in the violet-purple portion of the visible spectrum when fully warmed up. Adjust the field lens so that an image of the source is focused on the entrance slit. A trick for peaking up the alignment is to set the software to continuous scan and then maximize the spectral line intensities by adjusting the x-y translator holding the field lens. Adjust the spectrograph micrometer so that the strong green and yellow mercury lines will be centered on the CCD array. For a 1200 l/mm grating, the micrometer directly indicates the wavelength (nm) which will be centered on the array. For other grating densities, you must scale the micrometer reading by the ratio of the new grating density to 1200.

The Linespec software, shown in Fig 3, which controls the CCD interface runs only in Windows 98 so the computer must be booted into this OS. Run "Linespec" software from the PC desktop. After the introductory animation, the software will display three different graphs, "Reference", "Background", and "Sample" which are used for different types of spectroscopy beyond the scope of this lab. Select the "Reference" window by double clicking on it and from the drop down menus, configure the CCD head's integration time, sweep method and spectrum type (i.e. "Reference"). The full text of the software users guide is available from the software help menu and is also available in hard copy on the desk next to the PC. Please do not remove these manuals from the laboratory!

MERCURY CALIBRATION SPECTRUM

Acquire calibration data sets of the mercury spectrum, with and without the 1" circular UV glass safety filter (Thermo Oriel 6057). Explore the effects of input slit width, grating line density, and integration time on throughput, spectral resolution, and spectral bandpass. The acquired spectrum will probably show a profusion of lines - many more than the prominent yellow, green, blue and purple lines of the famous mercury spectrum. Several of the lines are, in fact, ultraviolet lines in the second-order spectrum, superimposed on the visible lines of the first-order spectrum. Your first job is to identify

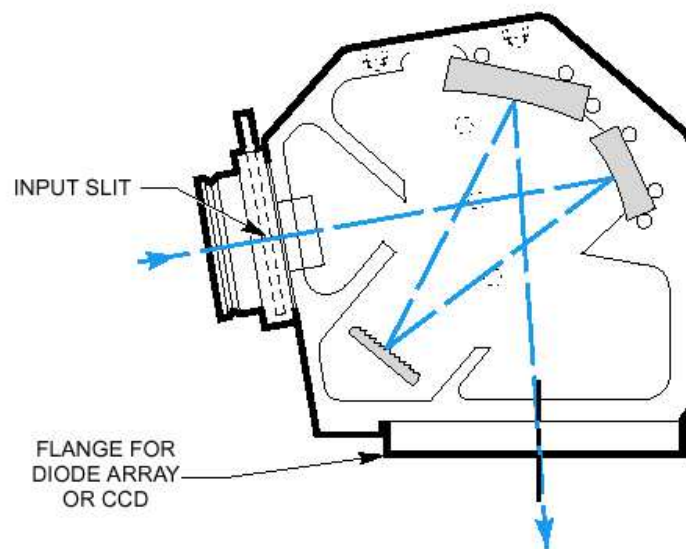


FIG. 1: Optical configuration of the MS125 Spectrograph in a Czerny-Turner mount. The plane grating provides dispersion and the concave mirrors provide focusing. Aberrations caused by the mirrors include astigmatism and spherical aberration. The grating measures $30\text{mm} \times 30\text{mm}$ square and the focal length of the first spherical concave mirror is 125mm . The output aperture is 25mm wide and is coupled to a linear CCD with 2048 elements, each $14\mu\text{m}$ high \times 200μ wide.

FIG. 2: The Linespec software interface to the Oriel MS125 Spectrograph.

all the lines with the aid of the mercury spectrum table in the CRC handbook. Later you will use the mercury spectrum as your calibrator for measurements of the hydrogen and sodium spectra.

Identify the lines by means of a bootstrap operation in which you first latch onto several of the most prominent lines, establish a tentative wavelength-position relation, and then see if the other fainter lines fall in place. The yellow doublet (5769.60 \AA and 5789.66 \AA) the green line (5460.74 \AA) and the purple line (4358.33 \AA) are particu-

larly useful landmarks within the mercury spectrum. It will help to make a plot of wavelength versus position. Look out for second order UV lines superposed on the first order visible spectrum (e.g. a 2500 Å line in second order would fall at exactly the same position as a 5000 Å line in first order). When you get it right, a plot of spectral wavelength position versus micrometer reading for all of the observed spectral lines should be very linear.

The Linespec software permits a software based wavelength calibration when 3 or more spectral lines have been identified. Once calibrated, you can change the x-axis units from pixel number to wavelength (nm), wavenumber (cm^{-1}) or eV. Note that once you have made a tentative polynomial fit, you can use the fitted formula to find the expected position of a line of specified wavelength, or the wavelength of a line at a specified position. This makes identification of the fainter lines easy, once you have established an accurate overall calibration.

Label as many of the transitions as you can with the aid of Figure 2.13 of Melissinos (in the figure caption “hydrogen” should be “mercury”). Note in particular the lines due to the interesting transitions $6^3D \rightarrow 6^1P$ for which $\Delta S=1$, and the 2536.5 Å line which is due to decay of the first excited state that is involved in the Franck-Hertz experiment. Check the validity of the dipole radiation selection rules.

Determine the number of lines mm^{-1} in the grating by measuring the linear separation of two identified lines of known wavelength on the acquired spectrum and applying the grating equation (see Appendix A).

HYDROGEN SPECTRUM – THE BALMER SERIES

The goals of this part of the experiment are:

1. to record the hydrogen spectrum at low and high resolutions together with a mercury calibration spectrum;
2. to identify and measure the wavelengths of the Balmer lines using a calibration based on mercury;
3. to compare the measured wavelengths with the Balmer formula, namely

$$\frac{1}{\lambda} = R_H \left(\frac{1}{n_f^2} - \frac{1}{n_i^2} \right) \quad (1)$$

where $n_f = 1, 2, 3, \dots$ and $n_i > n_f$. $n_f = 2$ corresponds to the Balmer series in the visible while $n_f = 1$ corresponds to the Lyman series in the UV.

4. to determine the value of the Rydberg constant, $R_H = 109,500 \text{ cm}^{-1}$

Acquire a series of hydrogen spectra with superimposed mercury calibration spectra, experimenting with resolution changes and integration times. Take care not to disturb the instrument between the hydrogen exposure and the mercury calibration exposure. Identify and measure as many of the Balmer lines as you can, comparing the wavelengths with those predicted by Equation 1. One way to do this is to compute a value of λ_0 for each of your measured Balmer lines, using in each case the appropriate values of n_f and n_i . From these data, determine a value and error for the Rydberg constant. You will probably observe other fainter features in the spectrum of the hydrogen discharge tube. Try to identify them.

SODIUM SPECTRUM – FINE STRUCTURE

The goals of this part of the experiment are:

1. to obtain a calibrated spectrum of sodium;
2. to measure the wavelengths of the lines and to measure their doublet separations;
3. to identify the transitions that give rise to the observed lines;
4. to determine the maximum energy of excitation of the sodium in the lamp.

The distortion of the $1/r$ field of the nucleus by the inner electrons has a substantial effect on the fine structure splittings of the $l > 0$ states that arise from the interaction between the magnetic moments associated with the spin and orbital angular moments of the optical electron. Where the fine structure splitting in hydrogen is very small and difficult to detect (0.08 Å in H_β), it is readily observed and measured in the alkali atoms. It decreases with n and l approximately as $1/[n^3l(1+l)]$, and so is most prominent in the P states. The splitting of the levels gives rise to a corresponding “doublet” structure of the spectral lines, with the most conspicuous effects occurring in the lines due to transitions to and from the P ($l = 1$) states. Doublets due to transitions that begin or end at a common state have identical energy separations. In the early days these separations provided important clues for identifying the transitions and deducing the level structure from observed spectra. See Melissinos for an energy level digram for sodium.

Obtain various sodium spectra of varying integration times with a superposed short mercury calibration spectrum, both with and without the UV filter. Determine the wavelengths of all the features of the spectrum.

Identify as many of the sodium lines as you can together with the initial and final atomic states of the transitions. Group them according to common final states and within each group compare the wavelengths with

those expected from energy levels given by the Rydberg formula

$$E = E_{\infty} - \frac{hcR}{(m + \mu)^2} \quad (2)$$

where m is an integer, and E and μ are constants.

Determine the fine-structure splittings of the $2P$ levels involved in the transitions responsible for the various doublets. Check whether the doublets originating from and terminating at the same $2P$ level have the same separation (in wave numbers). Determine the ratio of the doublet separations of the $3P$ and $4P$ levels, and compare with the semi-empirical rule that the ratio is proportional to $1/n^3$. Approach these measurements as an exercise in experimental accuracy and error estimation, and their interpretation as a challenge to your understanding of atomic structure.

You may find there are lines you cannot identify using only the sodium lines listed in the CRC Tables. Try to identify them, i.e. figure out what other element(s) may be in the lamp.

Measuring Isotopic Shifts in the Balmer Lines

In this part of the experiment you will determine the ratio of the deuteron mass to the proton mass by measuring the isotope shifts of the Balmer lines. Most of the differences in the energy levels of the hydrogen isotopes (hydrogen, deuterium, and tritium) arise from the differences in the reduced mass that occurs in the simple Bohr theory that explains the Balmer formula. (The differences due to interactions involving the nuclear magnetic moments are very much smaller in magnitude and not detectable with our instruments). With a little algebra the ratio of the deuteron mass to the proton mass can be expressed in terms of the wavelength λ of a Balmer line and its shift $\Delta\lambda$ between hydrogen and deuterium.

The measurement is performed with a high resolution scanning monochromator, a schematic diagram of which is shown in Fig. 4.

The monochromator has been painstakingly aligned. Please do not alter the arrangement of the optical components between the entrance and exit slits. You may adjust the other parts of the equipment, i.e. the slits themselves and the input optics which couple the light source to the input slit. If you suspect misalignment of the internal parts of the monochromator, ask for help.

HIGH-RESOLUTION MONOCHROMATOR

The monochromator is interfaced to a PC running Microsoft Windows and National Instruments LabVIEW software over a GPIB connection. A schematic of the instrument is shown in Figure 4.

The basic steps for using the instrument follow:

1. **At the end of your session, return the monochromator's grating to the zero position before shutting off the motor controller unit. Failure to do so will frustrate the calibration of the next group.**
2. Turn on the mercury discharge lamp and place it as close as possible to the input slit. It takes a few minutes for the discharge to stabilize.
3. Remove the small lid on the top of the monochromator to verify groove density of the installed gratings. The turret holds two gratings, either of which may be selected in software: Grating position '0' has 2400 grooves mm^{-1} at a blaze wavelength of 300nm while grating position '1' has 300 grooves mm^{-1} with a blaze wavelength of 600nm.
It is recommended that you start with the coarse 300 groove mm^{-1} grating in order to survey the broadest portion of the spectrum and explore the operation of the instrument before making your final measurements.
4. Turn on the Ministep Driver Unit (MSD-2) using the power switch on the back panel. You should hear a small clunk as the gear motor is engaged. Power cycling once or twice is sometimes necessary.
5. Boot the PC into Windows 2000, login as 'student'. The login process automatically loads LabVIEW and the monochromator control program shown in Figure 3. After the program is loaded, run the code by clicking on the white arrow in the upper left corner of the window. The main drop down menu bar contains various operations for controlling the monochromator. The first thing you should do is 'Establish GPIB Communication'. If communication is established between the MSD-2 and the PC, you will see the numbers '3.6' appear in the upper corners of the start-up window matrix. If after about 10 seconds the VI times out with no changes, try power cycling the MSD-2, and then retry establishing GPIB communication.
6. Select the desired turret position ('0' or '1') and then select 'Change Turret Position' from the drop down menu bar. Wait for the menu bar to revert back to 'Waiting for next command' before proceeding. You should execute this step even if the display 'reads' the correct position, as it needs to retrieve information about the grating's groove density.
7. Examine the mechanical counter on the side of the monochromator to see that it reads exactly 0.0. This counter can be used to determine

FIG. 3: The LabVIEW software interface to the Jobin-Yvon 1250M monochromator. Note that the user should always enter spectral units of Å while the ‘counter’ indicator will display the mechanical counter positions necessary to scan this portion of the spectrum. The limits of the instrument are 0 to 15,000 in mechanical counter units.

the current wavelength setting according to $\lambda = \text{counter} \times \frac{\text{installed grating density (lpmm)}}{1200 \text{ lpmm}}$. If not, select ‘Move grating to zero position’ from the menu bar.

8. Replace the lid with 4 screws above the turret grating assembly.
9. **Double check that the top of the monochromator is covered before turning on the high voltage to the photomultiplier tube as ambient light levels can damage a PMT biased at high voltages.** Set the high voltage to +950 VDC.
10. The input and output slits are controlled by micrometers. They can be set from 3 μm to 3mm. Set the width of both slits initially to be 1mm. **Do not attempt to adjust the micrometers to a width < 3 μm . This can damage the sensitive slits!** The height of the input slit is controlled by a sliding blade and should be set initially at 2mm.
11. The light ‘acceptance cone’ of the instrument is set by the size of the grating (110x100mm) and the distance from it to the input slit. For this instrument, the f -number = 11. If you find that you are light limited, try increasing the integration time or using a short focal length lens to form an image of the lamp at the entrance slit.

Your first task is to examine the instruments’ calibration. Plot the reading provided by the mechanical counter against wavelength to guide your subsequent work and reduce confusion as to where you are in the

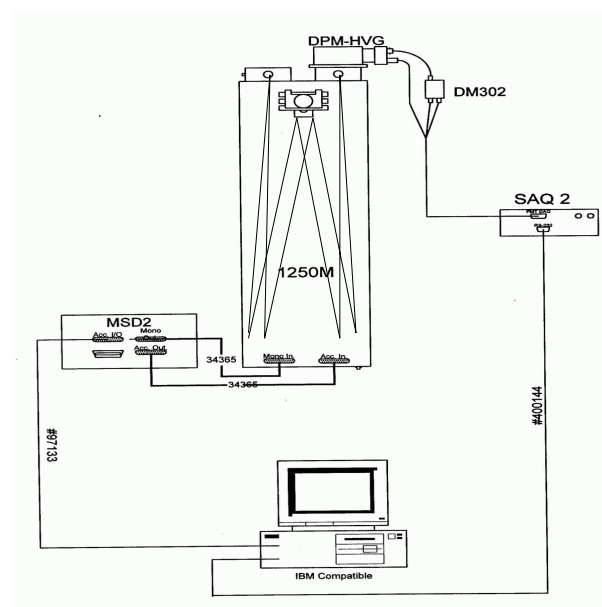


FIG. 4: Schematic of the Junior Lab high resolution monochromator.

spectral range. The mercury spectrum you obtained with the Thermo Oriel (low-resolution) grating spectrograph and the CRC table of mercury wavelengths should be used to aid in your identification of the lines detected by this higher resolution instrument.

The wavelength range of the monochromator is 0-15,000 units as displayed by the mechanical counter. The gratings are rotated by a spring-loaded lever set against the grating mount which is attached to a turret inside the instrument. **Please do not attempt to change the turrets yourself, since a slip may damage the very expensive gratings.**

Mount the mercury tube at a position such that the image cast by the field lens falls on the entrance slit of the spectrograph. With the entrance slit wide open at ~ 1 -3mm check that light is coming through the slit. When this condition is achieved, dispersed images of the slit (i.e. the spectral lines) should be formed in the plane of the exit slit. As the grating is rotated, the slit images will pass over the slit, causing the photomultiplier to register the presence of ‘spectral lines’ at various angular orientations of the grating as indicated on the mechanical counter. When you find a bright line, reduce the slit width to $\sim 100 \mu\text{m}$.

Once you have established the calibration, mount the H-D discharge tube, check that the image of the tube is focused on the entrance slit. Search for the H_{β} line(s) at the position expected from the calibration. When you find the line you should be able to observe the presence of the isotope-shifted line very nearby. Repeat for all the Balmer lines you can identify.

ANALYSIS

Compute the value of m_d/m_p and an error estimate from the measured separations of the hydrogen and deuterium Balmer lines, using the mercury calibration data. Compare the results with the known ratio of the atomic weights of deuterium and hydrogen.

SUGGESTED THEORETICAL TOPICS

1. Derivation of the grating equation.
2. Bohr theory of the hydrogen atom and the isotope shift.
3. Schrödinger theory of the hydrogen atom.
4. Fine structure.
5. The correspondence principle.

-
- [1] P. R. Bevington & D. K. Robinson 1992, Data Reduction and Error Analysis for the Physical Sciences, 2nd Edition, McGraw Hill.
 - [2] M. Born, M. 1969, Atomic Physics (Blackie & Sons Ltd).
 - [3] F. A. Jenkins & H. E. White, Fundamentals of Physical Optics (McGraw-Hill).
 - [4] A. C. Melissinos 1966, Experiments in Modern Physics (Academic Press).
 - [5] R. Rhodes 1986, The Making of the Atomic Bomb (Simon and Schuster).
 - [6] B. Rossi 1965, Optics (Addison-Wesley).
 - [7] C. F. White 1934, Introduction to Atomic Spectra (McGraw-Hill).

APPENDICES

GRATING PHYSICS

Figures 1 and 4 show the arrangement of optical components in both the spectrograph and monochromator. Note that the “source” for both these systems is a narrow slit upon which an external light source is focused. To understand the optics of any spectrograph or monochromator it is essential to realize that a narrow spectral “line” is actually a monochromatic image of the slit. Widen or lengthen the slit and you widen or lengthen the resulting spectral line. The width of a line depends on the width of the slit, the sharpness of the focus, and the intrinsic spectral width of the line, and the number of reflecting grooves of the grating that contribute to the total amplitude of the optical disturbance at the focal plane.

To understand the physics of both these instruments, envision spherical monochromatic light waves (i.e. “Huygens wavelets”) diverging from any given point at the slit and which are reflected by the collimating mirror into plane waves traveling toward the grating. Reflections from the grooves in the gratings form cylindrical wavelets which interfere constructively only in certain narrow ranges of directions so as to comprise, in effect, a set of plane waves each traveling in one of those directions. In the spectrograph, a second mirror acts to focus the incident plane waves upon the CCD array while in the monochromator it is the same mirror now acting as a camera mirror which focuses the incident plane waves to a diffracted image of the original slit at the focal plane of the monochromator where it then passes through an exit slit and onto the photocathode of a sensitive photomultiplier tube.

In both cases, the spectrum appears as monochromatic slit images spread out in the direction of dispersion of the grating. Also in both instruments, the bandpass spectrum is adjusted by rotating the grating about a vertical axis. They differ essentially in that the spectrograph captures all of the information simultaneously while the monochromator needs to be mechanically scanned over the entire bandpass region of interest to acquire the same information content.

The gratings used in both instruments are plane reflection gratings. In the spectrograph, the default grating (Oriel 77411) is a ruled grating with 1200 lines mm^{-1} and is blazed at 350nm (12.2°). The bandpass is $\sim 170\text{nm}$ and the ruled area is $30\text{mm} \times 30\text{mm}$.

The most general form of the plane reflection grating is shown in Figure 5. Each “tread” or “riser” of the staircase reflects a narrow rectangular piece of an incident plane wave, and this piece spreads about the specular reflection direction according to the principles of Fraunhofer diffraction. The resulting cylindrical wavelets may be thought of as combining at some distance to form

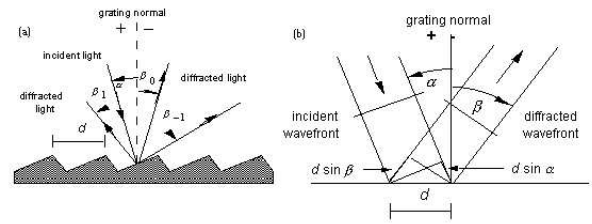


FIG. 5: Reflection Grating Geometry: (a) A beam of monochromatic light of wavelength λ is incident on a grating and diffracted along several discrete paths. (b) For planar wavefronts, The terms in the path difference, $d \sin \alpha$ and $d \sin \beta$, are shown. (From Thermo RGL Handbook)

diffracted plane waves with maximum intensities in directions such that the differences in path length along the reflected rays from successive grooves is an integral number of wavelengths. This condition is expressed by the grating equation

$$m\lambda = d(\sin \alpha + \sin \beta) \quad (3)$$

where α and β are the angles between the grating normal GN and the directions of incidence and reflection, respectively, d is the distance between grooves, and m is an integer called the “order” of the interference.

The angular dispersion produced by this grating is defined by the differential relation

$$\frac{d\beta}{d\lambda} = \frac{1}{d\lambda/d\beta} = \frac{m}{d \cos \beta} = \frac{\sin \alpha + \sin \beta}{\lambda \cos \beta} \quad (4)$$

For a given diffracted wavelength λ in order m (corresponding to an angle of diffraction β), it is convenient to characterize the reciprocal linear dispersion or plate factor P , usually measured in nm mm^{-1}

$$P = \frac{d \cos \beta}{mf} \quad (5)$$

where f is the effective focal length of the spectrograph (125mm for the Oriel MS125).

In the monochromator however, the grating is used in a Littrow Configuration where $\alpha = \beta$, and under these conditions Equation 3 simplifies to

$$m\lambda = 2d \sin \beta \quad (6)$$

Furthermore, Equation 4 becomes

$$D = \frac{d\beta}{d\lambda} = \frac{2}{\lambda} \tan \beta \quad (7)$$

When $|\beta|$ increases from 10° to 63° in Littrow use, the angular dispersion increases by a factor of ten, regardless

of the spectral order or wavelength under consideration. Once β has been determined, the choice must be made whether a fine-pitch grating (small d) should be used in a low order or a coarse-pitch grating (large d) such as an echelle grating should be used in a higher order. In this experiment, the former solution was chosen to provide a much larger free spectral range (see below).

At 4358 Å in first order (corresponding to $\beta = 31.5^\circ$ by Equation 6), the grating in our monochromator has dispersion of 2.8×10^{-4} radians Å⁻¹ using Equation 7. With a focusing mirror of focal length 1250mm following the grating, the linear dispersion would be 0.35 mm Å⁻¹, or about 20 times that of the Oriel MS125 grating spectrograph (~ 0.017 mm Å⁻¹).

The grating used in the Hydrogenic Spectroscopy experiment is ruled with 2400 lines mm⁻¹ ($d=4167$ Å). From Equation 6, light at 4358 Å will be refracted in first order at $\beta = 31.5^\circ$ in first order and at 63.0° in 2nd order. Light emitted at this latter angle will miss the focusing mirror and thus we are dealing with essentially just 1st order diffraction.

Finally, from Equation 6 we find that the difference between two wavelengths diffracted at the same angle in successive orders, called the free spectral range, is given by the equation

$$\lambda_1 + \Delta\lambda = \frac{m+1}{m}\lambda_1 \quad (8)$$

from which

$$F_\lambda = \Delta\lambda = \frac{\lambda_1}{m} \quad (9)$$

THE BOHR MODEL APPLIED TO THE VISIBLE SPECTRUM OF HYDROGEN

The hydrogen atom consists of a heavy proton of charge e and a much lighter $m_p/m_e = 1860$ electron of charge $-e$ that circles around it, held in orbit by the mutual attraction of opposite charges. During the latter half of the 19th century, scientists made many detailed measurements of the emission lines of atomic hydrogen. Many attempts were made to interpret their positions in the spectrum but none were successful until 1885 when Joannes Balmer noted that their wavelengths could be represented very simply by

$$\lambda = 3645.6n^2\left(\frac{1}{n^2} - 4\right)nm \quad (10)$$

In 1913, Niels Bohr proposed that electrons move in orbits whose angular momentum is quantized according to:

$$mvr = n\hbar \quad (11)$$

where $\hbar = 1.055 \times 10^{-27}$ erg s (6.58×10^{-22} MeV s). He also suggested that electrons can make transitions only

between these orbits and when doing so will emit (or absorb) radiation with frequency:

$$\nu = \frac{E_i - E_f}{h} \quad (12)$$

where $h = 2\pi\hbar$ and $E_{i,f}$ are the energies of the initial and final states.

Using these two quantization statements and assuming the special case of circular orbits, we may determine the electron energies by balancing the Coulomb attractive force with the centrifugal (repulsive) force:

$$\frac{mv^2}{r} = \frac{Ze^2}{r^2} \quad (13)$$

Combining Equations 11 and 13 yields:

$$v = \frac{Ze^2}{n\hbar} \quad (14)$$

and

$$r = \frac{n^2\hbar^2}{m_eZe^2} \quad (15)$$

If we now introduce the fine-structure constant $\alpha = \frac{e^2}{\hbar c} = \frac{1}{137}$, these can be expressed as

$$v = \frac{n^2\hbar}{\alpha Zm_e c} \quad (16)$$

and

$$r = \frac{n^2\hbar}{\alpha Zm_e c} = a_0 = 5.29\text{Å} \text{ for Hydrogen} \quad (17)$$

The total energy of the atomic system (kinetic and potential) is given by:

$$E = \frac{1}{2}mv^2 - \frac{Ze^2}{r} = \frac{Z^2\alpha^2(m_e c^2)}{2n^2} = \frac{13.6eV}{n^2} \quad (18)$$

where $\alpha = 1/137$ and $m_e c^2 = 511keV$ is the rest-mass of the electron. Figure 6 shows a cartoon of the Bohr atom and its predicted transitions.

ISOTOPIC FINE STRUCTURE: HYDROGEN-DEUTERIUM SHIFT

To account for the finite mass of a real hydrogen nucleus of mass M_n and electron of mass M_e as depicted in Figure 7 we must replace the mass of the electron m_e in Equation 18 by the reduced mass μ where $\frac{1}{\mu} = \frac{1}{m_e} + \frac{1}{m_n}$. The energy levels of Equation 18 now become

$$E = \frac{13.6eV}{n^2} \cdot \frac{1}{1 + M_e/M_n} \quad (19)$$

This results in a wavelength shift of 1 part in 3680 for each atomic transition (e.g. 1.32 Å for the $n=4$ to $n=2$ 4861 Å line).

FIG. 6: . An illustration of the Bohr model of the hydrogen atom showing the Lyman ($n_f = 1$, Ultraviolet), Balmer ($n_f = 2$, Visible) and Paschen ($n_f = 3$, Infrared) series. From [?]

SOLVING THE SCHRÖDINGER EQUATION FOR THE HYDROGEN ATOM

One can also derive the energy levels of the hydrogen atom using the *time-independent* Schrödinger equation. The basic equation of nonrelativistic quantum mechanics can be written in the form:

$$-\frac{\hbar^2}{2\mu}\nabla^2\Psi + V\Psi = E\Psi \quad (20)$$

or

$$H\Psi = E\Psi \quad (21)$$

where

$$H^0 = \frac{p^2}{2\mu} + \frac{e^2}{r} \quad (22)$$

is the Hamiltonian of the system and represents the total (kinetic plus potential) energy of the system and $E = \frac{Z^2\alpha^2\mu c^2}{2n^2}$ are the eigenvectors of the Hamiltonian (and which are equivalent to the Bohr Energies in Equation 18). The detailed solution to Equation 21 is presented in many textbooks, e.g. see [? ? ?]. Here we present a summary of the most important steps.

For the particular case of the spherical Coulomb potential in the hydrogen atom, we describe the wavefunction in spherical polar coordinates and separate the angular dependence from its radial dependence:

$$\Psi(r, \theta, \phi) = R(r)\Theta(\theta)\Phi(\phi) = R(r)Y(\theta, \phi) \quad (23)$$

FIG. 7: Revolution around the common center of mass. Since the nucleus is not infinitely heavy, it too moves very slightly. The problem can be simplified by changing the coordinates to the center of momentum reference frame in which the electron's mass is replaced by it's reduced mass. From [?].

The solutions of this separable equation are listed in Appendix . Here it is more illuminating to describe their general form:

$$\Phi_{m_l}(\phi) = e^{im_l\phi} \quad (24)$$

$$\Theta_{lm_l}(\theta) = \sin^{|m_l|} \cos \theta \quad \text{polynomial in } \theta \quad (25)$$

$$R_{nl}(r) = e^{-(\text{constant})r/nr^l} \quad \text{polynomial in } r \quad (26)$$

with the full normalized hydrogen wave functions given by [?]:

$$\psi_{nlm} = \sqrt{\left(\frac{2}{na}\right)^3 \frac{(n-l-1)!}{2n[(n+l)!]^3}} e^{-r/na} \left(\frac{2r}{na}\right)^l L_{n-l-1}^{2l+1} \left(\frac{2r}{na}\right) Y_l^m(\theta, \phi) \quad (27)$$

HYDROGEN FINE STRUCTURE CORRECTIONS

We can however introduce corrections (perturbations) to the Coulomb potential which allow us to more accurately describe the hydrogen spectrum. Fine structure perturbations to the Hamiltonian given in Equation 22 which change the energies by order $\alpha^4 mc^2$. These include:

1. relativistic correction due to the velocity of the electron, $\frac{v}{c} \approx \alpha = \frac{1}{137}$. The relativistic **kinetic** energy

is:

$$\sqrt{m^2c^4 + p^2c^2} - mc^2 = mc^2 + \frac{p^2}{2m} - \frac{p^4}{8m^3c^2} + \dots, \quad (28)$$

where we've assumed $pc \ll mc^2$ (i.e. $v \ll c$) and expanded the LHS in powers of the momentum \vec{p} . Thus $H_r = -\frac{p^4}{8m^3c^2}$. In 1st order perturbation theory, the correction to E_n is given by the expectation value of H' in the unperturbed state.

$$E_r^1 = -\frac{1}{8m^3c^2} \quad (29)$$

See [?] for details but after the dust clears:

$$E_r^1 = -\frac{E_n^2}{2mc^2} \left[\frac{4n}{l+1/2} - 3 \right] \quad (30)$$

- spin-orbit coupling between the intrinsic electron spin and the magnetic field in its vicinity caused by it's orbital motion about the nucleus. Recall that the energy of a magnetic dipole in a magnetic field is given by $E = -\vec{\mu} \cdot \vec{B} \implies H_{SO} = -\frac{1}{2}g\mu \cdot \vec{B}$ where $g = 2.00232$ is the "Lande g-factor" for the electron spin and the 1/2 corrects for Thomas precession. Quantum Mechanically, this coupling (also called LS Coupling) is given by:

$$H_{SO} = \frac{1}{2m^2c^2} \frac{1}{r} \frac{dV(r)}{dr} \vec{S} \cdot \vec{L} \quad (31)$$

The total angular momentum (\vec{J}) is the sum of that due to the electron's orbital motion about the nucleus (\vec{L}) and the intrinsic angular momentum of the electron due to it's spin (\vec{S}). They are added according to:

$$\vec{J} = \vec{L} + \vec{S} \quad (32)$$

$$\vec{J} \cdot \vec{J} = \vec{L} \cdot \vec{L} + \vec{S} \cdot \vec{S} + 2\vec{S} \cdot \vec{L} \quad (33)$$

$$\vec{S} \cdot \vec{L} = \frac{\vec{J} \cdot \vec{J} - \vec{L} \cdot \vec{L} - \vec{S} \cdot \vec{S}}{2} \quad (34)$$

and finally, using the allowable values for these quantities:

$$\vec{S} \cdot \vec{L} = \frac{\sqrt{j(j+1)} + \dots}{2} \quad (35)$$

The perturbing Hamiltonian may now be written as:

$$H_{FS} = H^0 + H_{SO} + H_r \quad (36)$$

After plenty of algebra and integrals, one arrives at the following result:

$$E_{n,j} = -\frac{13.6eV}{n^2} \left[1 + \frac{\alpha^2}{n^2} \cdot \left(\frac{n}{j+1/2} - \frac{3}{4} \right) \right] \quad (37)$$

which includes all of the known structure in the Hydrogen, see Figure 8. Not discussed here is the "Lamb-shift" which splits the $2S_{1/2}$ and $2P_{1/2}$ states and which is on the order of $\alpha^5 = 10^{-6}eV$. An understanding of the Lamb-shift requires quantum field theory [?].

FIG. 8: A comparison of the hydrogen energy levels predicted by Bohr theory and fine structure corrections for the relativistic motion of the electron and the spin-orbit coupling effect. $\bar{v} \equiv \frac{1}{\lambda} = \frac{E}{hc} \text{cm}^{-1}$. From reference [?].

HYDROGEN ATOM WAVE EQUATIONS

This separation is successful and results in an **angular wave equation** :

$$L^2 Y_l^m(\theta, \phi) = \hbar^2 l(l+1) Y_l^m(\theta, \phi) \quad (38)$$

with solutions given by spherical harmonics $Y_l^m(\theta, \phi)$, specified by the quantum numbers l and m_l with $m_l = 0, \pm 1, \pm 2, \dots, \pm l$. The eigenvectors for this equation are $\sqrt{l(l+1)}\hbar$.

The other separable part is the **radial wave equation**:

$$\frac{d^2(rR)}{dr^2} - \frac{2\mu}{\hbar^2} V r R = \frac{-2\mu E r R}{\hbar^2} \quad (39)$$

replace this with griffiths 4.53

where the potential is now given by:

$$V = \frac{-Ze^2}{r} + \frac{l(l+1)\hbar^2}{2\mu r^2} \quad (40)$$

The new effective potential contains a so-called centrifugal term that tends to throw the particle outward.

The radial wave equation has solutions $R_{n,l}(r)$ given by:

$$R_{nl} = \rho^l L_{nl}(\rho) e^{-\rho/2} \quad (41)$$

with $n = 1, 2, \dots$ and $l = 0, 1, 2, \dots, n - 1$. The variable ρ is proportional to the radius r :

$$\rho = \frac{2Z}{n} \times \frac{\mu}{m_e} \times \frac{r}{a_0} \quad (42)$$

where a_0 is the Bohr radius from Equation 17. The factor $L(\rho)$ is called an **associated Laguerre polynomial**. The solution of this equation results in E_n identical to those found by Bohr (though without his assumption of circular orbits).

From [?], the first few normalized hydrogen wave functions are:

$$(43)$$

EQUIPMENT LIST

Item	Model	Contact
Spectrograph	MS125	oriel.com/download/pdf/77400.pdf
1" UV Filter	6057	oriel.com
1" PCX Lenses	Various	thorlabs.com
Monochromator	1250M	jobinyvon.com
Photomultiplier Tube	R928	usa.hamamatsu.com/hcpdf/R928.pdf
H-D Spectral Lamps	Custom	electrotechnicalproduct.com
Spectral Lamps	Various	edmundscientific.com
Sodium Lamp	???	???
LabVIEW	Version 6.1	ni.com